iScience

CellPress
OPEN ACCESS

Article

Magnetoencephalographic spectral fingerprints differentiate evidence accumulation from saccadic motor preparation in perceptual decision-making

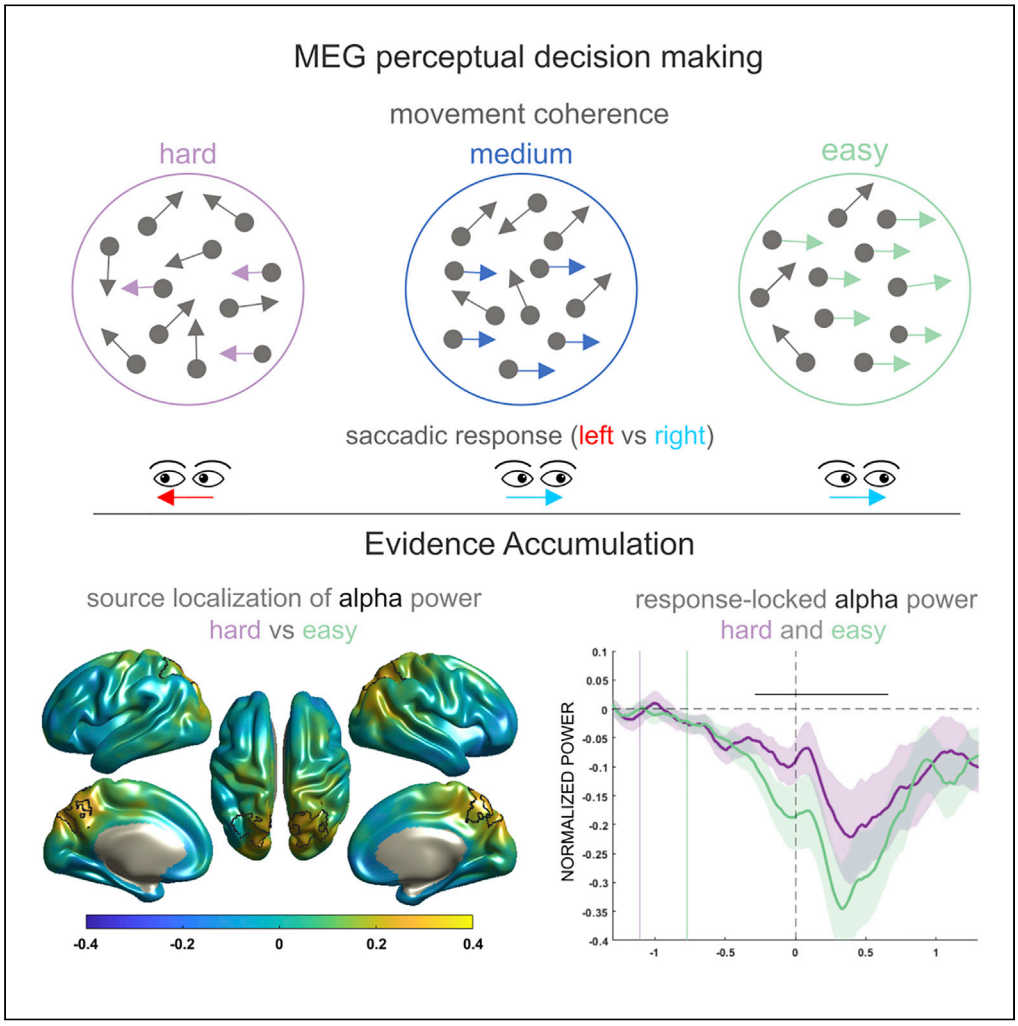

Antea D'Andrea, Alessio Basti, Annalisa Tosoni, ..., Gian Luca Romani, Vittorio Pizzella, Laura Marzetti

laura.marzetti@unich.it

Highlights

Continuous random dot motion paradigm offers a naturalistic view of decision-making

Parieto-occipital alpha band ERD underpins evidence accumulation predicting behavior

Parieto-occipital beta band oscillations support saccadic motor preparation

Spectral features disentangle functional roles in the intentional account model

D'Andrea et al., iScience 25, 105246
October 21, 2022
https://doi.org/10.1016/j.isci.2022.105246

iScience

CellPress
OPEN ACCESS

Article

Magnetoencephalographic spectral fingerprints differentiate evidence accumulation from saccadic motor preparation in perceptual decision-making

Antea D'Andrea,[1] Alessio Basti,[1] Annalisa Tosoni,[1] Roberto Guidotti,[1] Federico Chella,[1] Sebastian Michelmann,[3] Gian Luca Romani,[2] Vittorio Pizzella,[1,2] and Laura Marzetti[1,2,4,*]

SUMMARY

The understanding of the neurobiological basis of perceptual decision-making has been profoundly shaped by studies in the monkey brain in tandem with mathematical models, providing the basis for the formulation of an intentional account of decision-making. Although much progress has been made in human studies, a characterization of the neural underpinnings of an integrative mechanism, where evidence accumulation and the selection and execution of responses are carried out by the same system, remains challenging.

Here, by employing magnetoencephalographic recording in combination with an experimental protocol that measures saccadic response and leverages a systematic modulation of evidence levels, we obtained a spectral dissociation between evidence accumulation mechanisms and motor preparation within the same brain region.

Specifically, we show that within the dorsomedial parietal cortex alpha power modulation reflects the amount of sensory evidence available while beta power modulations reflect motor preparation, putatively representing the human homolog of the saccadic-related LIP region.

INTRODUCTION

Perceptual decision-making is classically defined as the ability to convert a sensory input from the external environment into an appropriate course of action (Rilling and Sanfey, 2011). Theoretical accounts have postulated an integrative mechanism of evidence accumulation toward a response-boundary as a basis for this sensory-motor transformation (Smith and Vickers, 1988). According to drift-diffusion models in particular, decisions are based on a mechanism of accumulation of (noisy) sensory information until a response boundary is reached; the rate of this evidence accumulation process increases as a function of the quality of information or sensory evidence extracted from the stimulus (Ratcliff and Smith, 2004; Ratcliff and McKoon, 2008).

Beyond theoretical implications, these models have been successfully used to interpret neurophysiological recordings in active-behaving monkeys that performed simple perceptual decision-making tasks (Gold and Shadlen 2007, review). For example, using a random dot motion (RDM) stimulus in which the direction of motion was indicated by a saccadic eye movement, Shadlen and colleagues (Shadlen and Newsome, 1996; Shadlen and Newsome, 2001) were able to show that both the monkey's behavioral performance and the firing rate of saccadic-related LIP neurons during the RDM task were well described by a boundary-crossing noisy accumulation process. Specifically, consistent with the representation of a decision variable that guides the transformation of sensory evidence into a motor response, a build-to-threshold ramp-like activity was observed in LIP neurons during perception of the RDM stimulus. Therein, the rate of that activity build-up was parametrically modulated by the variation in sensory evidence of the motion stimulus. These findings provided the basis for the formulation of an intentional account of decision-making, according to which decisions are represented in the same systems devoted to the planning/execution of the motor response, i.e., decisions are indivisible from the way they are reported (Shadlen et al., 2008).

Recently, several efforts to characterize the neural mechanisms of decision-making in the human brain have been undertaken (Meindertsma et al., 2017; Kelly and O'Connell, 2015). Applying analyses of

[1]Department of Neuroscience, Imaging and Clinical Sciences, University of Chieti-Pescara, Chieti, Italy

[2]Institute for Advanced Biomedical Technologies, University of Chieti-Pescara, Chieti, Italy

[3]Department of Psychology, Princeton University, Princeton, NJ, USA

[4]Lead contact

*Correspondence: laura.marzetti@unich.it

https://doi.org/10.1016/j.isci.2022.105246

single-trial EEG data, O'Connell and colleagues (2012) (O'Connell et al., 2012) were able to demonstrate a similar evidence accumulation process over time in human neural activity, leveraging the high temporal resolution afforded by EEG. Seminal fMRI studies have further shown that human decision-making hinges on modulation of activity in sensory-motor areas (Heekeren et al., 2004, 2008; Tosoni et al., 2008, 2014; Liu and Pleskac, 2011; Ploran et al., 2007). What is still missing is a succinct spatio-temporal characterization of this evidence accumulation process in humans, which can be addressed with MEG, an imaging method that can provide high temporal and spatial resolution.

The need for high spatiotemporal resolution in the characterization of neural underpinnings of decision-making is further highlighted by studies that investigate the spectral properties of perceptual detection tasks (Haegens et al., 2014, 2011; Spitzer and Blankenburg, 2011). Indeed, stimulus detection tasks have identified two functionally distinct neural correlates in the alpha and beta frequency bands, as they typically show an alpha power decrease and/or a beta power increase. The role of alpha band activity suppression is classically defined in terms of mechanisms of neural facilitation or engagement (D'Andrea et al., 2019; Jensen and Mazaheri, 2010) whereas the role of beta band activity is often interpreted in terms of recruitment of the sensorimotor system (Buchholz, 2014; Pfurtscheller and Lopes da Silva, 1999).

A key challenge that emerges from the nature of motor planning tasks in humans and non-human primates is that the motor response and the decision variable are typically correlated. This has made it notoriously difficult to arbitrate between neurophysiological correlates that are involved in evidence accumulation and motor preparation. Indeed, the distinct functional roles of alpha and beta oscillatory dynamics during the decision-making process still need clarification: it remains unanswered how the neural signals for the representation of a decision variable and the planning/execution of the selected responses reciprocally and continuously co-operate to generate appropriate behavior.

This issue is further exacerbated by the disruptive nature of hand motor responses on the MEG and EEG signals. Indeed, the hand motor responses might exhibit larger interference with our "signal of interest", i.e. alpha/beta band activity during the decision interval. A MEG study that leverages oculomotor responses can help reducing confounds in the result interpretation.

In this study, we apply a continuous version of the RDM decision-making task that is designed to investigate a freely evolving decision-making signals in a naturalistic view and to disentangle motor preparation processes from evidence accumulation processes.

By requiring participants to make a saccadic eye movement (leftward or rightward) under varying rates of evidence accumulation, we closely mirror paradigms that have been applied in studies on non-human primates.

This paradigm, together with the good spatial and high temporal resolution of MEG, made it possible to derive a characterization of evidence accumulation and motor preparation in time and space; our results demonstrate a spectral dissociation within the same cortical region between mechanism of evidence accumulation in the alpha band and a mechanism of saccadic planning, i.e., planning of the selected decision outcome, in the beta band.

RESULTS

MEG data were acquired from sixteen subjects performing a continuous version of the classical random dot motion task (Newsome et al., 1989) (Figure 1A). During the task, participants were instructed to maintain central fixation while monitoring a cloud of incoherently moving dots for intermittent targets. Targets were defined by 1.9 s periods of coherent motion in the leftward or rightward direction (30%, 60%, or 90% of motion coherence) within otherwise incoherent dot motion. Participants were instructed to detect these intermittent periods of coherence motion occurring every 3.3, 6.6, or 8.4 s on average within the RDM stimulus by performing a saccadic eye movement in the corresponding motion direction (i.e., leftward, rightward).

Data analysis at the behavioral level was conducted to determine the effect of sensory evidence (30%, 60%, or 90% of motion coherence) on accuracy and latency of the response times to the motion-direction target stimulus. Data analysis at the neural level investigated power modulations of the MEG signal as a function of sensory evidence.

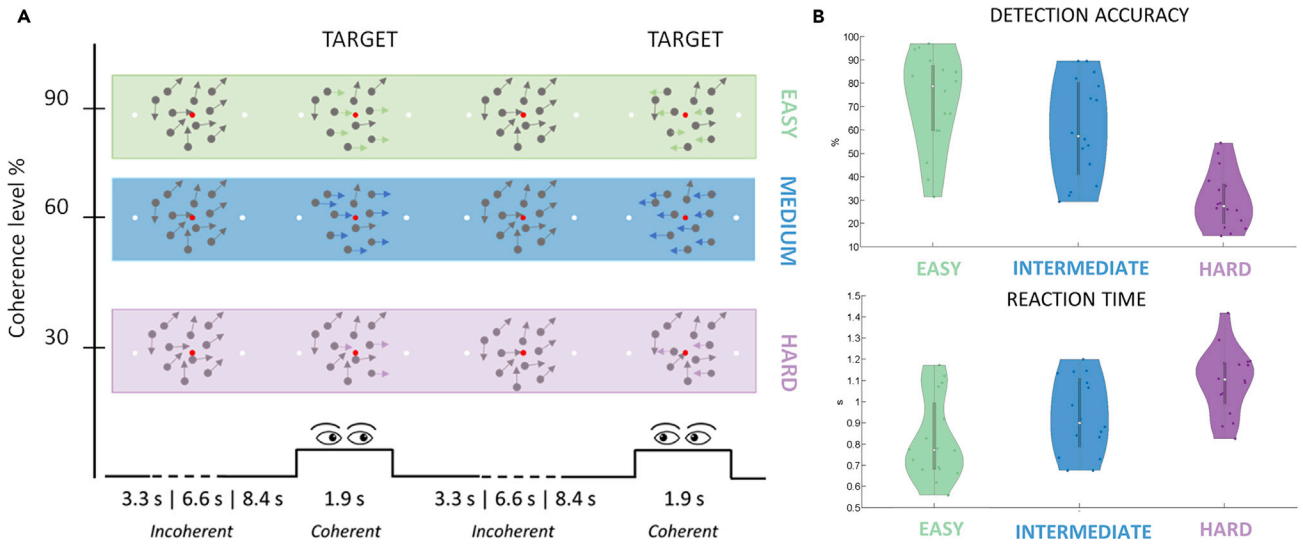

Figure 1. Paradigm and behavioral results

(A) Schematic illustration of one block of the continuous version of the random dot motion paradigm in which a cloud of incoherently moving dots is monitored by the subjects for intermittent targets of 1.9 s of coherent motion in the leftward or rightward direction. Participants indicate the leftward or rightward motion with a saccadic eye movement.

(B) Violin plots for (top) average across trials of detection accuracy, and (bottom) reaction time for each coherence level (easy, intermediate, hard); the white dot and the thick whiskers denote the median value across subjects and the range from the 25th to the 75th percentile, respectively. A significant main effect of evidence is observed on both measures of accuracy ($F(2,30) = 55.39$, $p < 0.00005$) and reaction time ($F(2,30) = 21.98$, $p < 0.00005$). The significant difference between all the conditions is confirmed by multiple comparison Bonferroni post-hoc tests (hard vs. intermediate vs. easy; accuracy: all $p < 0.02$; RTs: all $p < 0.04$).

Accuracy and reaction times are parametrically modulated by the sensory evidence

Assessment of the task's behavioral performance was based on analysis of the electro-oculographic (EOG) signal recorded during the RDM task (compare Methods). In particular, since a strong overlap (about 85%) was observed between target detection and target classification (i.e., correct detection vs. correct discrimination of the coherent motion target stimulus), task accuracy was defined on the basis of the percentage of correctly detected target stimuli. Target detection was classified according to the presence of a saccadic eye movement, i.e., sustained EOG amplitude modulations preceded by a rapid signal increase, during the 2150 ms interval from the target stimulus (i.e., coherent motion) presentation. Similarly, detection times were estimated by computing the time lag between the onset of the coherent target stimulus and the EOG amplitude modulation.

As displayed in Figure 1B, the results of EOG analysis indicate that both indices of performance are parametrically modulated by the level of sensory evidence informing the saccade. In particular, the behavioral results indicate that changes in detection accuracy followed changes in target evidence (range from 30% to 90% of coherent motion) employed in our study. Indeed, as shown by a repeated-measures ANOVA with sensory evidence (hard, intermediate, and easy) as a factor, the parametric modulation by the amount of sensory information informing the decision was statistically confirmed by a main effect of evidence on both indices of performance measures (accuracy: $F(2,30) = 55.39$, $p < 0.00005$; RT: $F(2,30) = 21.98$, $p < 0.00005$) and by a significant difference between all the conditions (multiple comparisons Bonferroni post-hoc tests; hard vs. intermediate vs. easy; accuracy: all $p < 0.02$; RTs: all $p < 0.04$).

Occipito-parietal regions exhibit an alpha band desynchronization during coherent motion

To explore the neural underpinnings of decision formation in this continuous detection paradigm, as a first step, we investigated frequency-specific power modulations associated with the intermediate condition, a condition that entails both an intermediate level of sensory stimulation and a corresponding behavioral performance, under the rationale that this condition acts as a spatial and temporal (frequency) "localizer".

To this end, a sensor-level time-frequency (TF) analysis was performed for each subject and valid response trials (i.e., target detection) in the post stimulus interval (0–2150 ms), time-locked to the target stimulus

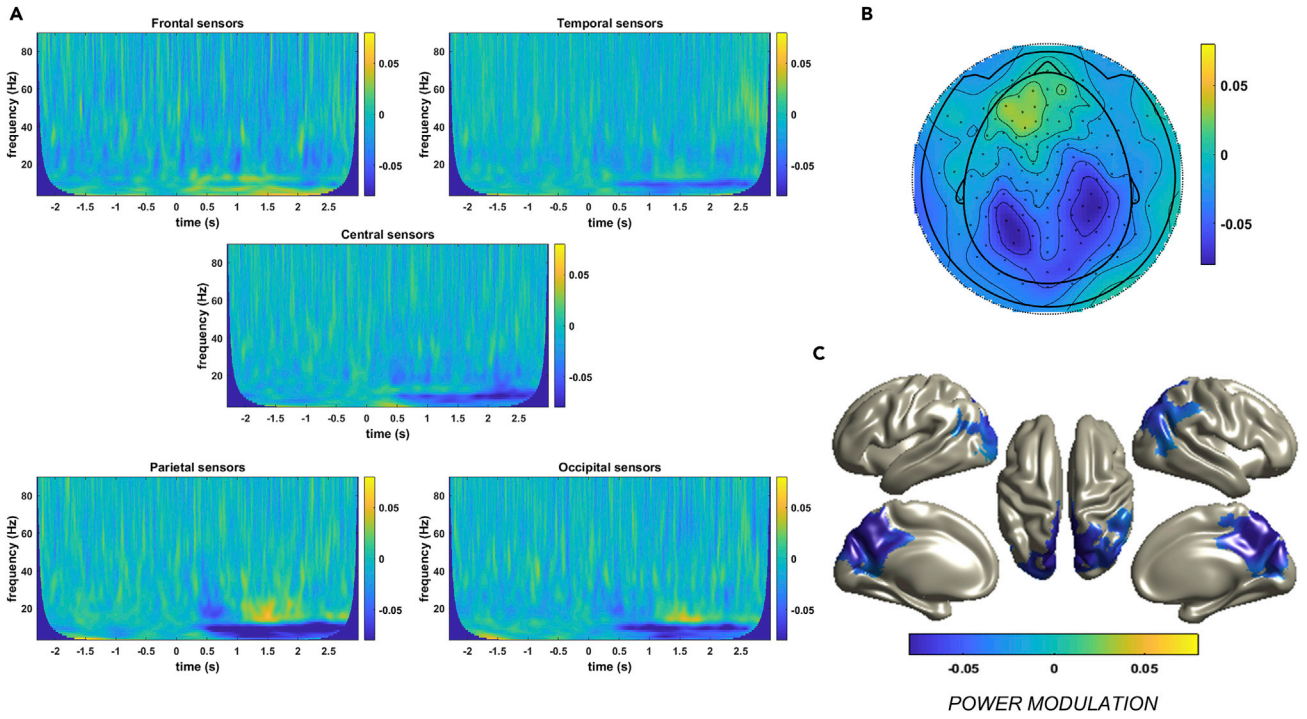

Figure 2. α band desynchronization locked to the target stimulus onset

(A) Group averaged time frequency (TF) plots of power modulations in the target interval (0–2150 ms) with respect to incoherent motion baseline (500 ms prior to the target stimulus onset) in the intermediate coherence level, averaged over frontal and temporal sensors (top), central sensors, and over parietal and occipital (bottom) sensors. On the x axis, time is represented such that zero corresponds to the target stimulus presentation.

(B) Group averaged topographical representation of significant alpha power decrease in the intermediate level versus baseline over the parieto-occipital regions.

(C) Group averaged source level representation of alpha band power decrease in the intermediate level versus baseline. The results of the permutation test based on pared-sample t-statistics, with cluster-based multiple comparison correction, show a sustained alpha power modulation (decrease), with respect to the baseline, specific for the parieto-occipital areas after the target stimulus presentation.

onset, and baseline corrected with respect to incoherent motion (500 ms interval prior to the target onset). As illustrated in Figures 2A and 2B, the results show a sustained alpha power modulation (8–12 Hz) over the occipital and parietal sensors. Since the analysis was conducted with respect to the baseline interval of incoherent motion direction, this modulation well qualifies as an event-related desynchronization (ERD) in the alpha band. Notably, in addition to the alpha ERD, the TF representation also shows a beta power modulation with respect to the baseline in the same interval. Specifically, a beta power ERD was also observed starting after the target stimulus onset (~500 ms) followed by a sustained beta event-related synchronization (ERS) in a typical ERD/ERS mode (Figure 2A).

To localize the cortical generators of the sustained alpha ERD modulation observed during presentation of the target stimulus, we next conducted a source reconstruction of the MEG signal using the exact low-resolution brain electromagnetic tomography (eLORETA) inverse method (Pascual-Marqui et al., 2011).

As displayed in Figure 2C, the results showed that the alpha band ERD observed during the post-stimulus interval was mostly localized in dorsomedial regions of the occipito-parietal cortex (permutation test based on paired-sample t-statistics with cluster-based multiple comparison correction). In particular, the activity modulation associated with perceptual decisions of intermediate difficulty (i.e., 60% accuracy) was most robustly observed in regions along the parieto-occipital sulcus (POs) and the precuneus extending laterally and dorsally into the intraparietal sulcus. Note that having taken into account the entire post-stimulus interval (0–2150 ms) could only have affected our results by weakening the statistical effect, whereas the fact that the effect is still significant means that it is strong and stable over time and across subjects.

Taking into account the target stimulus interval, the observed power modulation persisted over time including the saccadic response execution interval, thus possibly confounding the discrimination between

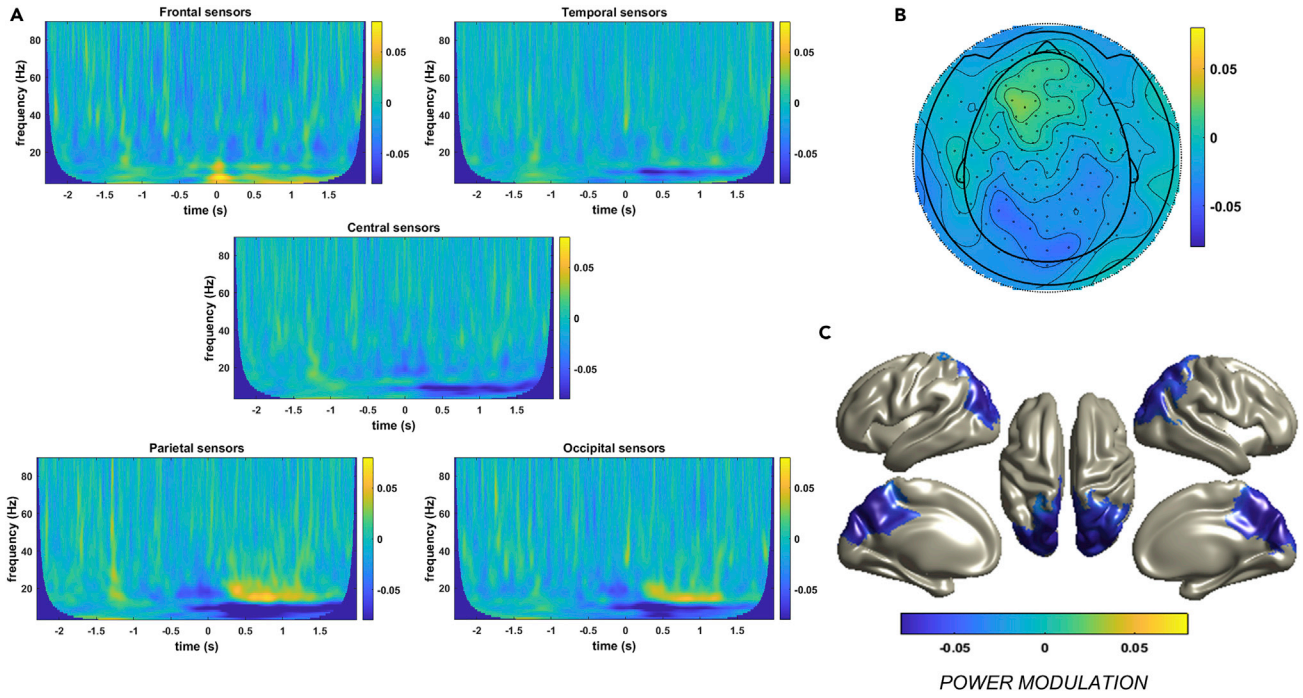

Figure 3. α band desynchronization locked to saccadic response onset

(A) Group averaged time frequency (TF) in the backward interval from response execution to stimulus onset corrected to baseline (500 ms prior to the stimulus onset) in the intermediate coherence level averaged over frontal and temporal sensors (top), central sensors (middle), and over parietal and occipital sensors (bottom). On the x axis, time is represented such that zero corresponds to the onset of the saccadic response.

(B) Group averaged topographical representation of significant alpha power decrease in the intermediate level versus baseline over the parieto-occipital regions.

(C) Group averaged source level representation of alpha band power decrease in the intermediate coherence level versus baseline. The results of the permutation test based on pared-sample t-statistics, with cluster-based multiple comparison correction, show that the sustained alpha power desynchronization, specific for the parieto-occipital sensors, occurs independently from the saccade execution.

oculomotor- vs. decision-related activity. To disentangle the two types of modulations, an additional TF analysis was conducted time-locking to the onset of the saccadic response. Specifically, a second time frequency analysis was conducted on the baseline corrected (500 ms interval prior to the target onset) backward interval from response execution to stimulus onset. As shown in Figure 3A, the results of this second analysis replicated the significant occipito-parietal alpha power desynchronization observed in the original TF analysis. The MEG source-level analysis (Figure 3C) further confirmed the cortical localization of this activity in dorsomedial regions of the occipito-parietal cortex (cluster-based multiple comparison correction) identified in the first source-level analysis. These results suggested that the alpha ERD observed in the interval of the motion target stimulus was unlikely to be explained by the motor component associated with execution of the saccadic response.

Finally, as for the alpha ERD modulation, the response-locked analysis on beta power modulations provided a replication of the results obtained in the corresponding forward analysis. Specifically, a typical beta ERD/ERS pattern was again observed in the backward interval from response execution, with a beta desynchronization followed by a sustained beta power synchronization after onset of the saccadic eye movement.

Alpha band modulation in parieto-occipital cortex underpins a behaviorally relevant evidence accumulation process

To explore the functional role of the previously observed alpha band power modulation, we used a sliding window approach to assess the alpha signal modulation and temporal evolution as a function of the two extreme evidence levels (easy vs. difficult decisions). This analysis was conducted in the parieto-occipital regions extending from parieto-occipital sulcus areas and dorsally to the intraparietal sulcus identified in the "localizer" source space analysis of power at the intermediate coherence level.

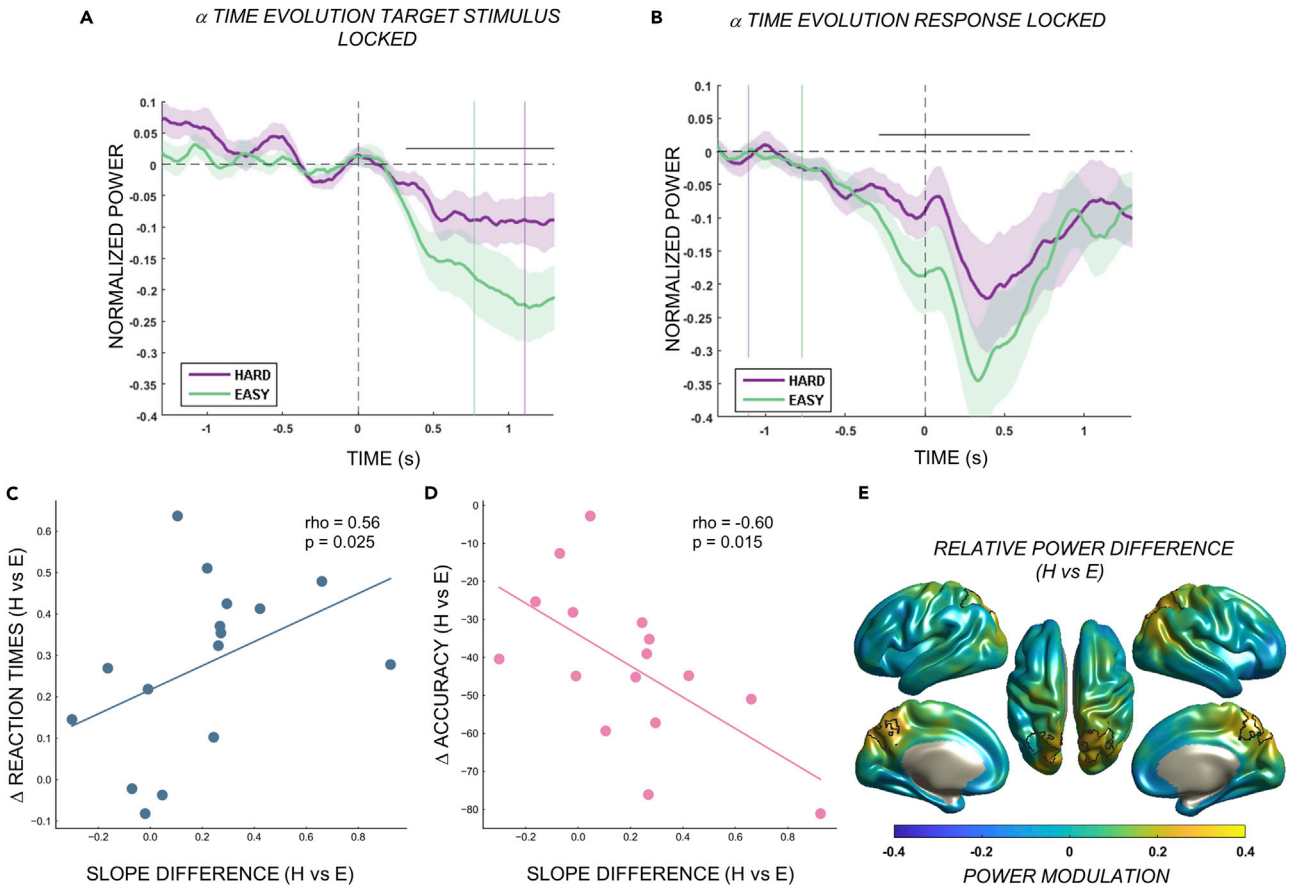

Figure 4. α band modulation reflects a sensory evidence accumulation process

(A) Time evolution of the alpha power modulation in the easy and hard coherence levels locked to the onset of the target stimulus in the dorsomedial regions of the occipito-parietal cortex. The plot highlights that in the easy level of the task (green trace), the alpha power ERD is larger with respect to the hard coherence level (violet trace). On the x axis, zero defines the onset of the stimulus presentation. The two traces significantly differ ($p = 2*10^{-4,}$ permutation test, with cluster-based multiple comparison correction) for a time range from 0.31 s to 1.32 s (indicated by the black horizontal solid line) after the target stimulus presentation. The vertical green and violet solid lines indicate the response time (average across subjects) in the easy and in the hard coherence levels, respectively; the shaded areas denote the standard error of the mean.

(B) Time evolution of the alpha power modulation in the easy and hard coherence levels locked to response onset (0s on the x axis) in the dorsomedial regions of the occipito-parietal cortex. The plot highlights that in the easy level of the task (green trace), the alpha power decrease is larger than in the hard coherence level (violet trace). The two traces significantly differ ($p = 0.003$, permutation test, with cluster-based multiple comparison correction) for a time range from −0.29 s before the onset of the saccadic execution to 0.77 s after the saccadic response execution (indicated by the black horizontal solid line). The vertical green and violet solid lines indicate the stimulus onset time (average across subjects) for the easy and in the hard condition, respectively; the shaded areas denote the standard error of the mean.

(C) Spearman correlation between the difference in the drift rate of the time evolution of alpha power modulation in the hard condition and the drift rate in the easy condition, and the difference of reaction times between the hard and the easy conditions. A significant positive correlation is observed (rho = 0.56, p = 0.025), indicating that subjects that feature a larger difference in reaction times (hard vs. easy) also feature a larger difference in the rate of reduction of alpha power (hard vs. easy).

(D) Spearman correlation between the difference the drift rate of the time evolution of alpha power in the hard condition and the drift rate in the easy condition, and the difference in the accuracy with which the task was performed in the hard condition with respect to the easy condition. A significant negative correlation is observed (rho = −0.60, p = 0.015), indicating that subjects that feature a larger difference in detection accuracy (hard vs. easy) also feature a larger difference in the rate of reduction of alpha power (hard vs. easy).

(E) Source-level representation of the alpha power difference in the hard versus easy condition. The map shows the source level representation of the difference between the alpha power decrease in the hard coherence level versus the easy coherence level, averaged in the time interval [-0.29 0] s where 0 s indicates the stimulus presentation. The black boundaries represent the bilateral saccadic related areas selected on the basis of an fMRI localizer task. The map shows that alpha power is higher in the hard coherence level with respect to the easy one in the lateral intraparietal regions

The occipito-parietal alpha power modulation during the hard and easy conditions, plotted as a function of time from the stimulus onset (t = 0 ms), is displayed in Figure 4A.

Notably, following an initial peak of activity observed soon after the onset of the coherent stimulation, which was common to both evidence levels, a progressive desynchronization (i.e., a power decrease) was observed during the target stimulus presentation, and thus during decision formation. The easy condition (Figure 4A, green line) displayed a significantly higher rate of alpha band desynchronization over time than the hard condition (Figure 4A, violet line), until the response was made (Figure 4A, green and violet vertical lines representing easy and hard conditions, respectively). A cluster-based permutation test, with a multiple comparison correction, confirmed the significantly larger desynchronization in the easy vs. hard condition ($p = 2*10^{-4}$).

Although the analysis of the temporal evolution of alpha band power modulation indicated that the divergence between the easy and the hard conditions was observed soon after target stimulus onset (significant difference starting at ~ 500 ms after the stimulus onset), the differential ERD associated with the two conditions persisted over time and included the interval of saccade execution. To disentangle the possible contribution of saccadic motor execution, an additional time-varying analysis on the alpha band ERD, time locked to the response execution, was conducted in the backward interval from saccadic response to stimulus onset. A significant difference between alpha power decrease elicited in the two levels of sensory evidence (easy, green line, vs. the hard condition, violet line) was observed over time (Figure 4B), as highlighted by a cluster-based permutation test (p = 0.003).

Taken together, these results support the hypothesis that the alpha desynchronization underpins an evidence accumulation mechanism related to decision-making process rather than an epiphenomenon correlated with saccadic execution.

This hypothesis was further corroborated by behavioral results, and by a linear regression fit aimed at identifying the slope of the time evolution modulations. To this end, we conducted a drift rate comparison test between the easy and hard conditions (paired-sample t-test between the drift rate in the two conditions and correlation with differences in behavioral performance). The results showed that the slope of the linear regression (R^2: median 0.50, interquartile range = 0.13–0.78 across subjects and conditions) for the time evolution of alpha power modulation was significantly larger in the easy condition as compared to the hard condition (p = 0.0206, paired-sample t-test, two-tail corrected). Crucially, at the group level, we observed a significant correlation with behavior, such that the difference in drift rate of the alpha power between the hard and easy condition was indicative of the subject's behavioral performance in the decision paradigm: subjects with a greater difference in drift rate between the easy and hard conditions also showed a greater difference in the accuracy and reaction time between the two conditions [reaction time: p = 0.024, rho = 0.56 (Figure 4C); detection accuracy: p = 0.015, rho = −0.60 (Figure 4D)].

To investigate the spatial specificity of the alpha band ERD difference between the easy and hard perceptual decision, we map this difference over the cortex; as displayed in Figure 4E, the alpha band ERD differences associated with hard vs. easy decisions localized in cortical regions spanning from the dorsal occipital cortex to the dorsomedial parietal cortex. Importantly, the source activity difference was observed in regions of the dorsal precuneus and posterior intraparietal sulcus closely overlapping with the definition of a saccadic-related posterior intraparietal region identified in previous fMRI studies using localizer scans of memory-guided pointing and saccadic eye movements (Tosoni et al., 2008, 2013) and here displayed by the black contour line.

Beta band oscillations support a motor preparation process

Several studies highlight the involvement of beta band oscillations in perceptual decision-making mechanisms, contributing to explain the role of oscillatory activity in the context dependency of stimulus processing (Haegens et al., 2014; Siegel et al., 2011).

As described above, in addition to the alpha ERD, our "localizer" sensor-level time-frequency analysis on the intermediate decision difficulty/sensory evidence condition also identified a beta band power modulation over the occipital and parietal sensors (Figure 2A). Specifically, a beta band power modulation was

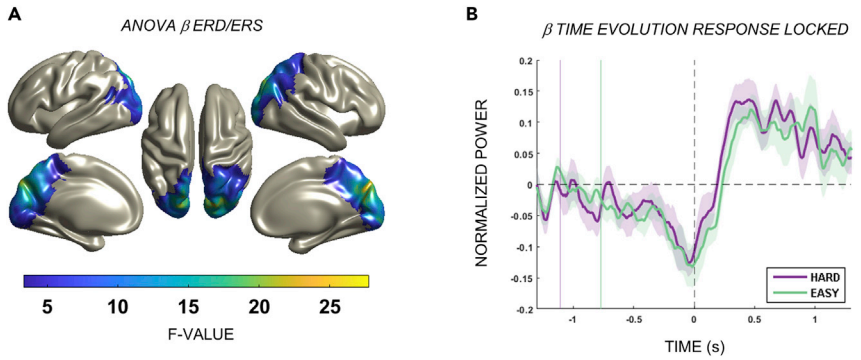

Figure 5. β band modulation reflects action preparation

(A) Cortical map of the F-value resulting from the one-way repeated-measure analysis of variance (ANOVA) with cluster-based multiple comparison correction, that contrasts beta power in the baseline interval (from 500 ms to 0 ms), ERD interval (from 350 ms to 850 ms), and ERS interval (from 1200 ms to 1700 ms). Time is locked to stimulus onset.

(B) Time evolution of the beta power modulation in the easy and hard coherence levels locked to response onset (corresponding to the 0 s in the x axis). In this plot, no significant difference emerged between the beta band power modulation in the easy condition (green curve) and the hard condition (violet curve). The vertical green and violet lines indicate the stimulus onset in easy and hard conditions respectively; the shaded areas denote the standard error of the mean.

identified during the interval of the target stimulus presentation, with a power decrease (ERD) starting soon after the target stimulus onset (from 350 ms to 850 ms) and a sustained power increase (ERS) after the onset of the saccadic eye movement (from 1200 ms to 1700 ms) in a typical ERD/ERS pattern.

A one-way repeated-measure analysis of variance (ANOVA), conducted on the intermediate difficulty level, contrasting the power in the baseline interval (from −500 ms to 0 ms; locked to the stimulus onset) and the power in the ERD/ERS intervals (ERD: from 350 ms to 850 ms; ERS: from 1200 ms to 1700 ms; locked to the stimulus onset) confirmed that, for hit trials, the beta band power modulation localized in posterior areas of the parieto-occipital cortex (Figure 5A). The comparison test on beta power modulations during the ERD/ERS intervals vs. baseline was conducted using a permutation test with cluster-based multiple comparison correction.

Finally, to further address the functional role of the beta band power modulation in the decision mechanism and to disentangle its contribution in motor preparation of the selected response, we assessed the beta power evolution over time as a function of the two extreme evidence levels (easy vs. hard conditions) in the backward interval from saccadic execution to stimulus onset. Time-varying modulations of cortical beta power for easy and hard conditions were assessed using a 350-ms-length sliding window approach, baseline corrected. The contrast between time-evolution modulations in the two conditions was conducted using a permutation test based on a paired-sample t-statistics with cluster-based multiple comparison correction.

As illustrated in Figure 5B, the results showed no significant variation of the beta band power modulation as a function of the decision difficulty level in the backward interval from saccadic execution. Specifically, a progressive activity decrease was observed for both conditions during the interval of the target stimulus presentation (green vertical line for easy condition and violet vertical line for hard condition) with a negative peak at the time of saccadic execution (t = 0).

Additionally, at group level, no significant correlation was found between the hard vs. easy beta power drift rate difference and the behavioral performance (reaction time: $p = 0.9847$, $rho = -0.0052$; detection accuracy: $p = 0.1295$, $rho = 0.3954$), providing corroborating evidence that beta power modulation does not play a role in the decision formation process.

Notably, the negative peak of the beta band power modulation observed at the time of saccadic execution was followed by an activity burst and a sustained power modulation during the time interval of saccade

execution. These results support the hypothesis that beta band power modulation reflects a frequency-specific mechanism of motor preparation and execution, occurring in the same brain areas in which alpha band desynchronization tracks a decision variable that accumulates evidence over time.

Note that we did not investigate effects in other frequency bands since the time-frequency analysis, spanning from 3 to 100 Hz, did not show any modulation in frequency bands different from alpha and beta (sign test, Bonferroni corrected).

DISCUSSION

The decision-making process has been described as an integrative mechanism of evidence accumulation toward a response-boundary (Smith and Vickers, 1988). Here, we present a spatiotemporal characterization of this decision-making process: in line with an intentional account of perceptual decision-making, we describe a spectral dissociation of a decision variable and a motor response within the same sensory-motor systems.

Specifically, we used a seamless random dot motion paradigm directly derived from monkey neurophysiological studies, in which the direction of motion was indicated by a saccadic eye movement. This allowed a naturalistic investigation of a freely evolving MEG signal that integrates sensory evidence over time. The results obtained using this paradigm suggest that the process of evidence accumulation for perceptual decisions is subserved by a power desynchronization mechanism in the alpha band (8–12 Hz), the rate of which depends on the quality of information extracted from the stimulus. In accordance with the prediction of the intentional model of decision-making, that postulates a representation of the decision variable in the same systems devoted to the planning of the motor response (Shadlen and Newsome, 1996 2001), we found that the alpha band power desynchronization occurred in parieto-occipital regions closely overlapping with saccadic areas classically associated with an oculomotor decision process (Tosoni et al., 2008). Critically, our results also show that the rate of alpha desynchronization in these regions was significantly larger during easy vs. difficult perceptual decision, which qualifies alpha power desynchronization as a neural counterpart of the evidence accumulation process. This is in line with a neurobiological framework that suggests low-frequency power decrease, such as alpha ERD, to represent a release from inhibition (Jensen and Mazaheri, 2010) that is associated with increased neuronal excitability (Samaha et al., 2020). Specifically, our results corroborate the hypothesis that alpha band modulations represent a liberal perceptual strategy (Haegens et al., 2014), a process that by increasing the desynchronization, and thus increasing the release from inhibition, effectively leads to a better performance with more detections of the target stimulus.

Indeed, at the group level, the difference in temporal evolution of alpha desynchronization between the easy and the hard perceptual condition tracked participants' behavioral performance. This was evident in detection accuracy and reaction times, which suggests that alpha power decreases optimize the sensory evidence accumulation process, facilitate a decision formation, and ultimately lead to an action execution.

Consistent with previous neurophysiological evidence of alpha power decrease and beta power increase during detection tasks (Donner et al., 2009; Haegens et al., 2011; Spitzer and Blankenburg, 2011), our results showed that in the posterior areas of the parieto-occipital lobe, the alpha power decrease was coupled with a beta band power modulation. Specifically, we observed a beta power decrease starting soon after the target stimulus onset, followed by a sustained power increase occurring after the onset of the saccadic response. In contrast to previous studies in which the contribution of the motor activity on perceptual decision processing was not fully clarified (Donner et al., 2008; Kloosterman et al., 2015b), our results describe a beta power modulation over time that reflects a frequency-specific mechanism of motor preparation and execution.

Overall, our results show a spectral dissociation between critical components of the decision process within the same cortical region. Alpha band desynchronization reflects the coding of a decision variable whereas beta band ERD/ERS is associated with motor components of the decision response.

The continuous paradigm used in this study allows the investigation of freely time-evolving decision-making variables, thus making it possible to study decision-making behavior in a dynamic and naturalistic manner. One of the advantages of naturalistic stimuli is their capability to elicit highly reproducible brain responses (Hasson et al., 2004). Prospectively, this reproducibility will be crucial to exploit neurostimulation

techniques for the study of psychological functions (Pitcher et al., 2021) and, thus, to improve the understanding of the decision-making process.

Finally, our study, while showing that the decision-related process and the motor preparation originate in the same cortical regions, disentangles neuronal populations that synchronize at different frequencies and subserve different functional roles. In turn, this knowledge is valuable for targeting the (parietal) cortex with non-invasive human brain stimulation protocols aimed at driving such distinct neural populations by a periodic external drive (Thut et al., 2011) and, thus, at selectively interfering with various cognitive processes. Indeed, modulation of brain oscillations in a controlled manner, such as that achievable with closed-loop stimulation protocols, would also be valuable for promoting brain function in therapeutic intervention.

Limitations of the study

This study contains possible limitations. The small number of miss trials in the easy level of coherence and, moreover, the different number of overall hit and miss trials does not allow to disclose a significant difference between those trials. Indeed, a two-way ANOVA with factors: coherence level (Hard vs. Easy) and detected coherent movement (Hit vs. Misses) returned a significant main effect of coherence level ($F(1,15) = 20.8$, $p = 0.00038$) but only a close to significance interaction effect between the two factors ($F(1, 15) = 4.32$, $p = 0.055$).

Additionally, although we decided to use saccadic eye movement to indicate the prevalent motion direction, thus minimizing the interference of the beta hand response on the decisional signals, a control group using a button press response could have been used to strengthen the interpretation of the results, consistently with the intentional account of decision-making model.

Finally, a fit of the alpha power time-course on the drift diffusion model (Ratcliff and McKoon, 2008) could have confirmed that alpha band modulation reflects a sensory evidence accumulation process.

STAR★METHODS

Detailed methods are provided in the online version of this paper and include the following:

- KEY RESOURCES TABLE
- RESOURCE AVAILABILITY
  - Lead contact
  - Materials availability
  - Data and code availability
- EXPERIMENTAL MODEL AND SUBJECT DETAILS
  - Human subjects
- METHOD DETAILS
  - Behavioral paradigm
  - Data collection
  - Behavioral data analysis
  - MEG data analysis

ACKNOWLEDGMENTS

This study was funded by the European Research Council (ERC Synergy) under the European Union's Horizon 2020 research and innovation programme (ConnectToBrain; grant agreement No. 810377). The content of this article reflects only the authors' view and the ERC Executive Agency is not responsible for the content. Author L.M. was also supported by Bial Foundation grant numbers 66/16 and 80/20.

AUTHOR CONTRIBUTIONS

A.D.A.: Conceptualization, investigation, formal analysis, writing - original draft, visualization; A.B.: methodology, software, formal analysis, visualization; A.T.: Conceptualization, writing - original draft, writing - review & editing; R.G.: software, visualization, writing - review & editing; F.C.: software, formal analysis; S.M.: writing - original draft, writing - review & editing; G.L.R.: funding acquisition, writing - review & editing; V.P.: methodology, writing - original draft, writing - review & editing; L.M.: methodology, writing - original draft, writing - review & editing, supervision.

DECLARATION OF INTERESTS

The authors declare no conflicts of interest.

INCLUSION AND DIVERSITY

We support inclusive, diverse, and equitable conduct of research.

Received: March 16, 2022
Revised: July 12, 2022
Accepted: September 27, 2022
Published: October 21, 2022

REFERENCES

Buchholz, V.N., Jensen, O., and Medendorp, W.P. (2014). Different roles of alpha and beta band oscillations in anticipatory sensorimotor gating. Front. Hum. Neurosci. *8*, 446. https://doi.org/10.3389/fnhum.2014.00446.

Dale, A.M., Fischl, B., and Sereno, M.I. (1999). Cortical surface-based analysis. I. Segmentation and surface reconstruction. Neuroimage *9*, 179–194. https://doi.org/10.1006/nimg.1998.0395. Fine modulo.

D'Andrea, A., Chella, F., Marshall, T.R., Pizzella, V., Romani, G.L., Jensen, O., and Marzetti, L. (2019). Alpha and alpha-beta phase synchronization mediate the recruitment of the visuospatial attention network through the Superior Longitudinal Fasciculus. Neuroimage *188*, 722–732. https://doi.org/10.1016/j.neuroimage.2018.12.056.

Donner, T.H., Sagi, D., Bonneh, Y.S., and Heeger, D.J. (2008). Opposite neural signatures of motion-induced blindness in human dorsal and ventral visual cortex. J. Neurosci. *28*, 10298–10310.

Donner, T.H., Siegel, M., Fries, P., and Engel, A.K. (2009). Buildup of choice-predictive activity in human motor cortex during perceptual decision making. Curr. Biol. *19*, 1581–1585. https://doi.org/10.1016/j.cub.2009.07.06.

Fischl, B. (2012). FreeSurfer. Neuroimage *62*, 774–781. https://doi.org/10.1016/j.neuroimage.2012.01.021.

Fischl, B., Sereno, M.I., Tootell, R.B., and Dale, A.M. (1999). High-resolution intersubject averaging and a coordinate system for the cortical surface. Hum. Brain Mapp. *8*, 272–284.

Gold, J.I., and Shadlen, M.N. (2007). The neural basis of decision making. Annu. Rev. Neurosci. *30*, 535–574. https://doi.org/10.1146/annurev.neuro.29.051605.113038.

Gramfort, A., Papadopoulo, T., Olivi, E., and Clerc, M. (2010). OpenMEEG: opensource software for quasistatic bioelectromagnetics. Biomed. Eng. Online *9*, 45. https://doi.org/10.1186/1475-925X-9-45.

Haegens, S., Nácher, V., Luna, R., Romo, R., and Jensen, O. (2011). Alpha oscillations in the monkey sensorimotor network influence discrimination performance by rhythmical inhibition of neuronal spiking. Proc. Natl. Acad. Sci. USA *108*, 19377–19382.

Haegens, S., Vázquez, Y., Zainos, A., Alvarez, M., Jensen, O., and Romo, R. (2014). Thalamocortical rhythms during a vibrotactile detection task. Proc. Natl. Acad. Sci. USA *111*, E1797–E1805. https://doi.org/10.1073/pnas.1405516111.

Hasson, U., Nir, Y., Levy, I., Fuhrmann, G., and Malach, R. (2004). Intersubject synchronization of cortical activity during natural vision. Science *303*, 1634–1640. https://doi.org/10.1126/science.1089506.

Heekeren, H.R., Marrett, S., and Ungerleider, L.G. (2008). The neural systems that mediate human perceptual decision making. Nat. Rev. Neurosci. *9*, 467–479. https://doi.org/10.1038/nrn237.

Heekeren, H.R., Marrett, S., Bandettini, P.A., and Ungerleider, L.G. (2004). A general mechanism for perceptual decision-making in thehuman brain. Nature *431*, 859–862. https://doi.org/10.1038/nature02966.

Jensen, O., and Mazaheri, A. (2010). Shaping functional architecture by oscillatory alpha activity:Gating by inhibition. Front. Hum. Neurosci. *4*, 186.

Kelly, S.P., and O'Connell, R.G. (2015). The neural processes underlying perceptual decision making in humans: recent progress and future directions. J. Physiol. Paris *109*, 27–37. https://doi.org/10.1016/j.jphysparis.2014.08.003.

Kleiner, M., Brainard, D., Pelli, D., Ingling, A., Murray, R., and Broussard, C. (2007). What's new in psychtoolbox-3. Perception *36*, 1–16. https://doi.org/10.1068/v070821.

Kloosterman, N.A., Meindertsma, T., Hillebrand, A., van Dijk, B.W., Lamme, V.A.F., and Donner, T.H. (2015b). Top-down modulation in human visual cortex predicts the stability of a perceptual illusion. J. Neurophysiol. *113*, 1063–1076.

Liu, T., and Pleskac, T.J. (2011). Neural correlates of evidence accumulation in a perceptual decision task. J. Neurophysiol. *106*, 2383–2398. https://doi.org/10.1152/jn.00413.2011.

Marcus, D.S., Harwell, J., Olsen, T., Hodge, M., Glasser, M.F., Prior, F., Jenkinson, M., Laumann, T., Curtiss, S.W., and Van Essen, D.C. (2011). Informatics and data mining tools and strategies for the human connectome project. Front. Neuroinform. *5*, 4. https://doi.org/10.3389/fninf.2011.00004.

Maris, E., and Oostenveld, R. (2007). Nonparametric statistical testing of EEG- and MEG-data. J. Neurosci. Methods *164*, 177–190. https://doi.org/10.1016/j.jneumeth.2007.03.024.

Meindertsma, T., Kloosterman, N.A., Nolte, G., Engel, A.K., and Donner, T.H. (2017). Multiple transient signals in human visual cortex associated with an elementary decision. J. Neurosci. *37*, 5744–5757. https://doi.org/10.1523/JNEUROSCI.3835-16.2017.

Newsome, W.T., Britten, K.H., and Movshon, J.A. (1989). Neuronal correlates of a perceptual decision. Nature *341*, 52–54. https://doi.org/10.1038/341052a0.

O'Connell, R.G., Dockree, P.M., and Kelly, S.P. (2012). Asupramodal accumulation to bound signal that determines perceptual decisions in humans. Nat. Neurosci. *15*, 1729–1735. https://doi.org/10.1038/nn.3248.

Oostenveld, R., Fries, P., Maris, E., and Schoffelen, J.M. (2011). FieldTrip: open source software for advanced analysis of MEG, EEG, and invasive electrophysiological data. Comput. Intell. Neurosci. *2011*. https://doi.org/10.1155/2011/156869.

Pascual-Marqui, R.D., Lehmann, D., Koukkou, M., Kochi, K., Anderer, P., Saletu, B., Tanaka, H., Hirata, K., John, E.R., Prichep, L., et al. (2011). Assessing interactions in the brain with exact low-resolution electromagnetic tomography. Philos. Trans. A Math. Phys. Eng. Sci. *369*, 3768–3784. https://doi.org/10.1098/rsta.2011.0081.

Percival, D.B., and Walden, A.T. (1993). Analysis for Physical Applica- Tions: Multitaper and Conventional Univariate Techniques (Cambridge University Press).

Pfurtscheller, G., and Lopes da Silva, F.,H. (1999). Event-related EEG/MEG synchronization and desynchronization: basic principles. Clin. Neurophysiol. *110*, 1842–1857. https://doi.org/10.1016/s1388-2457(99)00141-8.

Pitcher, D., Parkin, B., and Walsh, V. (2021). Transcranial magnetic stimulation and the understanding of behavior. Annu. Rev. Psychol. *72*, 97–121. https://doi.org/10.1146/annurev-psych-081120-013144.

Pizzella, V., Penna, S.D., Gratta, C.D., and Romani, G.L. (2001). SQUID systems for biomagnetic imaging. Supercond. Sci. Technol. *14*, R79–R114. https://doi.org/10.1088/0953-2048/14/7/201.

Ploran, E.J., Nelson, S.M., Velanova, K., Donaldson, D.I., Petersen, S.E., and Wheeler, M.E. (2007). Evidence accumulation and the moment of recognition: dissociating perceptual recognition processes using fMRI. J. Neurosci. *27*, 11912–11924. https://doi.org/10.1523/JNEUROSCI.3522-07.2007.

Ratcliff, R., and McKoon, G. (2008). The diffusion decision model: theory and data for two-choice decision tasks. Neural Comput. *20*, 873–922. https://doi.org/10.1162/neco.2008.12-06-420.

Ratcliff, R., and Smith, P.L. (2004). A comparison of sequential sampling models for two-choice reaction time. Psychol. Rev. *111*, 333–367. https://doi.org/10.1037/0033-295X.111.2.333.

Rilling, J.K., and Sanfey, A.G. (2011). The neuroscience of social decision-making. Annu. Rev. Psychol. *62*, 23–48. https://doi.org/10.1146/annurev.psych.121208.131647.

Samaha, J., Iemi, L., Haegens, S., and Busch, N.A. (2020). Spontaneous brain oscillations and perceptual decision-making. Trends Cogn. Sci. *24*, 639–653.

Shadlen, M.N., and Newsome, W.T. (2001). Neural basis of a perceptual decision in the parietal cortex (area LIP) of the rhesus monkey. J. Neurophysiol. *86*, 1916–1936. https://doi.org/10.1152/jn.2001.86.4.1916.

Shadlen, M.N., Kiani, R., Hanks, T.D., and Churchland, A.K. (2008). Neurobiology of decision making: An intentional framework. In C. Engel & W. Singer (Eds.), Better than conscious? Decision making, the human mind, and implications for institutions (MIT Press), pp. 71–101.

Shadlen, M.N., and Newsome, W.T. (1996). Motion perception: seeing and deciding. Proc. Natl. Acad. Sci. USA *93*, 628–633. https://doi.org/10.1073/pnas.93.2.628.

Siegel, M., Engel, A.,K., and Donner, T.,H. (2011). Cortical network dynamics of perceptual decision- making in the human brain. Front. Hum. Neurosci. *5*, 21. https://doi.org/10.3389/fnhum.2011.00021.

Smith, P.L., and Vickers, D. (1988). The accumulator model of two-choice discrimination. J. Math. Psychol. *32*, 135–168. https://doi.org/10.1016/0022-2496(88)90043-0.

Spitzer, B., and Blankenburg, F. (2011). Stimulus-dependent EEG activity reflects internal updating of tactile working memory in humans. Proc. Natl. Acad. Sci. USA *108*, 8444–8449.

Thut, G., Schyns, P.G., Gross, J., and Gross, J. (2011). Entrainment of perceptually relevant brain oscillations by non-invasive rhythmic stimulation of the human brain. Front. Psychol. *2*, 170. https://doi.org/10.3389/fpsyg.2011.00170.

Tosoni, A., Corbetta, M., Calluso, C., Committeri, G., Pezzulo, G., Romani, G.L., and Galati, G. (2014). Decision and action planning signals in human posterior parietal cortex during delayed perceptual choices. Eur. J. Neurosci. *39*, 1370–1383. https://doi.org/10.1111/ejn.12511.

Tosoni, A., Galati, G., Romani, G.L., and Corbetta, M. (2008). Sensory-motor mechanisms in human parietal cortex underlie arbitrary visual decisions. Nat. Neurosci. *11*, 1446–1453. https://doi.org/10.1038/nn.2221.

Tosoni, A., Shulman, G.L., Pope, A.L., Mc Avoy, M.P., and Corbetta, M. (2013). Distinct representations for shifts of spatial attention and changes of reward contingencies in the human brain. Cortex. https://doi.org/10.1016/j.cortex.2012.03.022.

STAR★METHODS

KEY RESOURCES TABLE

REAGENT or RESOURCE	SOURCE	IDENTIFIER
Software and algorithms		
Fieldtrip v2020103	Oostenveld et al. (2011)	https://www.fieldtriptoolbox.org/download
Original Code		https://github.com/mambolab/perceptual-decision-making
MATLAB vR2019	MathWorks	https://www.mathworks.com/products/matlab.html
Analyzed magnetoencephalographic data	This paper	https://doi.org/10.5281/zenodo.6861111
Behavioral data	This paper	https://doi.org/10.5281/zenodo.6861111

RESOURCE AVAILABILITY

Lead contact

Further information and requests for resources and reagents should be directed to and will be fulfilled by the lead contact, Prof. Laura Marzetti (laura.marzetti@unich.it).

Materials availability

This study did not generate new unique reagents.

Data and code availability

- Raw data reported in this paper will be shared by the lead contact upon request.
- Analyzed magnetoencephalographic data and behavioral data has been deposited at Zenodo and is publicly available as of the date of publication. DOIs are listed in the key resources table.
- Original code has been deposited at GitHub and is publicly available as of the date of publication. DOIs are listed in the key resources table.
- Any additional information required to reanalyze the data reported in this paper is available from the lead contact upon request.

EXPERIMENTAL MODEL AND SUBJECT DETAILS

Human subjects

Sixteen subjects (age 23.31 $\pm$ 1.57, 14 females, and 2 males) with no previous history of neurological or psychiatric diseases were enrolled in this study. All subjects provided written informed consent. Experiments were carried out in accordance with the Declaration of Helsinki and all recruitment and assessment procedures were approved by the Ethical Committee of the University of Chieti-Pescara.

METHOD DETAILS

Behavioral paradigm

Task design

A continuous version of the classical Random Dot Motion task (Newsome et al., 1989) was implemented using Psychtoolbox (Kleiner et al., 2007) (Figure 1A). In this visual perceptual decision-making task, while fixating on a central red circle, subjects monitored a cloud of dots moving incoherently for intermittent targets defined by 1.9 s periods of coherent motion in the leftward or rightward direction. Incoherently moving dots were continuously displayed during an inter-target interval of different duration that randomly varies between 3.3 s, 6.6 s and 8.4 s. Participants were not aware about either the inter-target duration or about its random variation. The percentage of coherently moving was randomly varied between 90%, 60% and 30% of motion coherence respectively defining the three conditions of sensory evidence or decision difficulty (i.e. easy, intermediate and hard). Motion direction and coherence level were changed independently and randomly on a target-by-target basis. Participants were trained to indicate the leftward or rightward direction of motion as soon as they perceived it by making a saccadic eye movement toward the

corresponding direction. The target of the saccadic eye movement was indicated by a white dot on the left/right edge of the screen (Figure 1A). The design included 14 task blocks with 24 target stimuli each (average duration 3.5 min) interleaved by one minute rest blocks, for a total of 336 target stimuli and a total task duration of about one hour.

Data collection

After standard screening procedures for magnetoencephalographic (MEG) and structural Magnetic Resonance Imaging (MRI), all subjects underwent MEG measurements while performing the continuous Random Dot Motion Task.

MEG data were recorded by the 153-channel MEG system installed at the Institute for Advanced Biomedical Technologies (ITAB) - University of Chieti-Pescara. This system includes 153 dc-SQUID integrated magnetometers arranged on a helmet covering the whole head (Pizzella et al., 2001). Electrocardiogram (ECG) and both vertical and horizontal electrooculogram (EOG) signals were recorded for artifact rejection and for monitoring the saccadic response. All signals were band-pass filtered at 0.16–250 Hz and sampled at 1 kHz. All participants also underwent structural MRI. The high-resolution structural volume was acquired with a 3 T Philips Achieva scanner at ITAB, via a 3D fast field echo T1-weighted sequence (voxel size 1 mm^3 isotropic, TR/TE =8.1/3.7 ms; flip angle 8°). In separate days prior to MEG recordings, the subjects performed training in a mock MEG session within the MEG environment to be able to respond via a clear horizontal saccadic movement, i.e., a saccadic eye movement towards left or right for leftward or rightward dots motion, respectively.

Behavioral data analysis

Behavioral performance during the task was assessed both in terms of accuracy in the target detection task and reaction times. Target detections were classified according to the presence of a saccadic eye movement during the 2150 ms interval from the target stimulus (i.e., coherent motion) presentation. A saccadic movement was defined as a rapid EOG (horizontal derivation) signal increase, defined as the saccade onset, followed by a sustained EOG signal amplitude. Saccadic moments were automatically identified by a specifically developed algorithm based on a 200-ms sliding window approach taking into account the mean amplitude of the signal within the window of interest (coherent motion), and its first discrete derivative. Two thresholds for mean amplitude and first derivative, respectively, were defined by analyzing the horizontal saccades, which was done by four independent raters; an expert operator double-checked saccade definitions.

A detected saccade was considered as a valid response if its onset was within 250 ms from the target offset. Detection accuracy was defined as the percentage of valid responses over the total number of targets. Reaction time was defined as the time interval, in seconds, between the target stimulus onset and saccade onset. A 3 × 2 ANOVA was used to examine statistical differences in detection accuracy and reaction time between the three evidence conditions.

MEG data analysis

Data preprocessing

MEG data for each subject were first preprocessed to exclude trials containing flux jumps of the detector, muscular activity, and eye blinks. Independent Component Analysis (ICA), implemented in the FieldTrip Matlab toolbox (Oostenveld et al., 2011), was run after trial exclusion to remove other biological and instrumental artifacts. Note that, among these, ocular artifacts were carefully removed from the MEG signal. This, together with saccade amplitude control in the experimental design makes it unlikely that confounds from saccade strength had an influence on the results. Cleaned data were then used for all subsequent analyses.

Sensor level analysis

To identify which frequency bands are involved in the perceptual decision-making process, i.e., which frequency bands show the strongest power modulation with respect to baseline, a sensor-level time-frequency (TF) analysis was performed for each subject for data from the intermediate coherence level (60% coherence). The intermediate condition was chosen *a priori* as a reference condition to identify frequency bands of interest. The easy and hand conditions were used to investigate power modulations. TF analyses were conducted by locking to the onset of the stimulus target (i.e., stimulus-locked) or to

the onset of the saccadic response (i.e., response-locked) with a baseline of 500 ms prior to the stimulus target onset.

To obtain TF power modulations at group level, we first realigned individual MEG channel positions to a standard layout, using the FieldTrip toolbox, to avoid mismatch of channel positions among subjects. After realignment, TF analysis was performed by using – for each frequency – a time window containing 5 cycles of that frequency. We then averaged the (logarithmically transformed) TF values across subjects and, finally, we averaged together groups of channels divided according to their spatial position (frontal, central, temporal, parietal, occipital).

Alpha band source space analysis

MEG source-level analysis was performed to assess alpha-band (8–12 Hz) cortical activity modulations locked to either the stimulus target onset or the response onset. Data segments for the intermediate condition level were considered from the post-stimulus interval and the pre-stimulus interval as baseline. In the stimulus-locked analysis, the post-stimulus interval ranged from 0 ms (i.e., stimulus target onset) to 2150 ms (i.e., stimulus target offset), while the pre-stimulus interval ranged from −2150 ms to 0 ms. In the response-locked analysis, the former interval ranged from −500 ms to 0 ms prior to the saccadic response, while the latter interval ranged from 500 ms to 0 ms prior to the stimulus target onset. Sensor-level cross-spectral density matrices in the alpha-band were computed using Slepian tapers with a 10 Hz center frequency to produce 2 Hz frequency smoothing (Percival and Walden, 1993). From these matrices, source level alpha power was estimated using the exact low resolution brain electromagnetic tomography (eLORETA) inverse method (Pascual-Marqui et al., 2011) for cortical sources located at 14,387 nodes of a triangulated mesh covering the midthickness surface (i.e., a surface halfway between the pial and white matter surfaces).

To allow direct averaging across subjects, single-subject midthickness surface meshes were surface-registered to a common template. This was achieved by first extracting highly dense cortical meshes from individual T1w MRI using Freesurfer (Dale et al., 1999; Fischl, 2012; Fischl et al., 1999), followed by mesh downsampling and template matching using the Human Connectome Project (HCP) workbench scripts available in FieldTrip (Marcus et al., 2011). Realistically shaped three-shell volume conductor models (scalp, skull, and intracranial volume) were constructed from the segmentation of T1w MR images. The MEG forward problem was solved using a Boundary Element Method (Gramfort et al., 2010). Within-subject modulations of cortical activity were assessed by contrasting the (logarithmically transformed) power in the post-stimulus interval with the power in the pre-stimulus interval using a permutation test based on pared-sample t-statistics (10,000 random permutations) with cluster-based multiple comparison correction (Maris and Oostenveld, 2007).

Time-varying modulations of cortical alpha power for easy (90% coherence) and hard (30% coherence) conditions were assessed using a sliding window approach. Specifically, cortical alpha power was calculated within a 350 ms window sliding for the whole data. This window length resulted into a 3 Hz smoothing around 10 Hz. A baseline correction was performed by subtracting the average (logarithmically transformed) power in the pre-stimulus interval.

The contrast between time-varying modulations in the easy and hard conditions was performed using a permutation test based on a paired-sample t-statistics (10,000 random permutations) with cluster-based multiple comparison correction. The same analysis pipeline was also used to assess time-varying modulations during missed trials. Finally, the drift rate of the time-varying modulations was evaluated through a linear regression fit in the post-stimulus interval. A paired-sample t-test was used to assess the drift rate differences between the easy- and hard condition.

Beta-band source space analysis

Two data segments from the post-stimulus interval (ERD: from 350 ms to 850 ms; ERS: from 1200 ms to 1700 ms; locked to the stimulus onset) and one data segment from the pre-stimulus interval (baseline, from 500 ms to 0 ms; locked to the stimulus onset) were considered for the intermediate condition level. Sensor-level cross-spectral density matrices were computed using Slepian tapers with a 19 Hz center frequency to produce 6 Hz frequency smoothing. Beta-band cortical power was computed from these matrices by using the eLORETA method. The comparison of cortical power in the baseline, ERD and

ERS intervals was performed by using a permutation test based on a one-way repeated-measure analysis of variance (ANOVA), with cluster-based multiple comparison correction.

Time-varying modulations of cortical beta power for easy and hard conditions were assessed using a 350-ms-length sliding window approach. A baseline correction was performed by subtracting the average (logarithmically transformed) power in the pre-stimulus interval. The contrast between time-varying modulations in the two conditions was performed by using a permutation test based on a paired-sample t-statistics (10,000 random permutations) with cluster-based multiple comparison correction.